JOURNAL OF GEOPHYSICAL RESEARCH, VOL. 100, NO. C3, PAGES 4977–4983, MARCH 15, 1995

Higher-order spectral analysis of nonlinear ocean surface gravity waves

Steve Elgar,[1] T.H.C. Herbers,[2] Vinod Chandran,[3] R.T. Guza [4]

Abstract. Bispectral and trispectral analyses are used to detect secondary and tertiary wave components resulting from nonlinear interactions among large-amplitude ocean surface gravity waves in 8- and 13-m water depths. Bispectra of bottom-pressure measurements indicate forced secondary waves at frequencies $2f_p$ about twice the primary power spectral peak frequency f_p. However, the interpretation of the bispectrum at sum frequencies of approximately $3f_p$ is ambiguous because contributions of both secondary and tertiary forced waves may be significant. Trispectral analysis confirms the presence of tertiary waves with frequency approximately $3f_p$. In 8 m depth the tertiary bottom-pressure field is dominated by interactions between three colinearly propagating wind-wave components with frequencies close to f_p. In 13 m depth these relatively short-wavelength forced waves are strongly attenuated at the seafloor and the tertiary wave field is driven by interactions between the dominant waves at f_p and obliquely propagating higher-frequency wind waves. The phases of the higher-order spectra are consistent with weakly nonlinear wave theory (Hasselmann, 1962).

Introduction

The local nonlinearity of ocean surface gravity waves is important to sediment transport [*Bowen*, 1980], the interpretation of remote sensing data [*Barrick and Lipa*, 1986], and the generation of seafloor microseisms [*Longuet-Higgins*, 1950] and infragravity waves [e.g., *Longuet-Higgins and Stewart*, 1964]. Perturbation expansion solutions to the equations of motion predict that nonresonant nonlinear interactions between freely propagating waves (obeying the linear dispersion relation) excite forced waves not obeying the linear dispersion relation (*Phillips*, [1960]; *Hasselmann*, [1962]; and many others). Although the effects of forced secondary waves excited by interactions between two wind-wave components are generally well understood, little is known about the existence and importance of tertiary waves forced by the interaction of three primary waves.

In the present study, higher-order spectral analysis is used to detect the presence of secondary and tertiary forced waves associated with the nonlinearity of energetic swell observed in 8- and 13-m water depths. Higher-order spectral analysis techniques are first described and then applied to the field data, followed by a summary of the results.

[1] School of Electrical Engineering and Computer Science, Washington State University, Pullman.

[2] Department of Oceanography, Naval Postgraduate School, Monterey, California.

[3] School of Electrical and Electronic Engineering, Queensland University, Brisbane, Australia.

[4] Center for Coastal Studies, University of California, La Jolla.

Paper number 94JC02900.
0148-0227/95/94JC-02900$05.00

Higher-Order Spectral Analysis of Nonlinear Waves

Conventional power spectral analysis cannot detect relatively weak forced waves submerged in a background of more energetic freely propagating wind waves. However, the phase coupling between the primary wind waves and associated forced waves is apparent in higher-order spectra [*Hasselmann et al.*, 1963]. The discrete power spectrum is defined here as

$$P(f_1) = E[A_{f_1} A^*_{f_1}] \tag{1}$$

where A_{f_1} is the discrete Fourier transform at frequency f_1, the asterisk indicates complex conjugation, and $E[]$ represents averaging. The bispectrum $B(f_1, f_2)$ [*Hasselmann et al.*, 1963; *Haubrich*, 1965; *Kim and Powers*, 1979] and trispectrum $T(f_1, f_2, f_3)$ [*Elgar and Chandran*, 1993; *Chandran and Elgar*, 1994, and references therein] are defined analogously as

$$B(f_1, f_2) = E[A_{f_1} A_{f_2} A^*_{f_1+f_2}] \tag{2}$$

$$T(f_1, f_2, f_3) = E[A_{f_1} A_{f_2} A_{f_3} A^*_{f_1+f_2+f_3}]. \tag{3}$$

Although the statistics of power spectra are well known and bispectral statistics are approximately known [*Brillinger and Rosenblatt*, 1967; *Elgar and Sebert*, 1989; *Chandran and Elgar*, 1991; and references therein],

trispectral statistics have only recently been studied in detail [see *Chandran et al.*, 1994; and references therein]. For a given number of degrees of freedom (dof) the statistical uncertainty of higher-order spectral estimates is larger than for power spectra.

For a weakly nonlinear wave field the Fourier amplitude A_f can be expressed as a perturbation expansion

$$A_f = \sum_{n=1}^{\infty} A_f^n \tag{4}$$

with A_f^1 the lowest order $O(\epsilon)$ (where ϵ is the nonlinear perturbation parameter) free wave Fourier amplitude, and A_f^n $(n > 1)$ the amplitude of the n^{th}-order $O(\epsilon^n)$ forced wave excited by interactions between n free wave components. Substitution of (4) into (2) and (3) yields

$$B(f_1, f_2) = \sum_{p=1}^{\infty}\sum_{q=1}^{\infty}\sum_{r=1}^{\infty} E[A_{f_1}^p A_{f_2}^q A_{f_1+f_2}^{r*}] \tag{5}$$

$$T(f_1, f_2, f_3) = \sum_{p=1}^{\infty}\sum_{q=1}^{\infty}\sum_{r=1}^{\infty}\sum_{s=1}^{\infty} E[A_{f_1}^p A_{f_2}^q A_{f_3}^r A_{f_1+f_2+f_3}^{s*}]. \tag{6}$$

Assuming that the wind-generated primary wave field is Gaussian, the lowest order terms in (5) and (6) ($O(\epsilon^3)$ and $O(\epsilon^4)$, respectively) vanish, as do all odd-order terms [*Hasselmann et al.*, 1963]. The lowest order ($O(\epsilon^4)$) nonzero contributions to the bispectrum result from phase coupling between two primary waves (each of $O(\epsilon)$) and a forced secondary wave (of $O(\epsilon^2)$) ($A^1A^1A^2$ products in (5)). In deep water ($kh \gg 1$, where k is the wavenumber and h is the water depth), forced wave amplitudes are usually much smaller than free wave amplitudes and are thus difficult to detect [*Donelan et al.*, 1985]. However, the relatively larger secondary waves in shallow and intermediate water depths have been studied extensively with the bispectrum, and observations compare well with theory [*Hasselmann et al.*, 1963; *Elgar and Guza*, 1985, 1986; *Herbers and Guza*, 1991, 1992, 1994; *Herbers et al.*, 1992, 1994]. The lowest order ($O(\epsilon^6)$) nonzero contributions to the trispectrum result from phase coupling between three primary waves and a tertiary wave ($A^1A^1A^1A^3$ products in (6)) or between two primary waves and two secondary waves ($A^1A^1A^2A^2$ products in (6)). Bispectral and trispectral analyses are used below to detect forced secondary and tertiary waves in seafloor pressure fluctuations observed in 8- and 13-m water depths during a storm.

Observations

The experiment site, near Duck, North Carolina, is offshore of a relatively straight barrier island and is exposed to the open ocean (see *Elgar et al.* [1992] and *Herbers et al.* [1994] for details). Bottom-pressure measurements were obtained in 8- and 13-m water depths, about 1 and 2 km from shore, respectively, during a northeaster on October 26, 1990. Sustained winds measured on a nearby pier were greater than 25 m/s with gusts up to 40 m/s. Wave breaking was extensive (Figure 1), and the significant wave height decreased from 5 to 4 m between 13- and 8-m water depths. The maximum spectral density of the bottom-pressure observations occurred at primary power spectral peak frequency $f_p = 0.11$ Hz, and in 8 m depth bumps at harmonic frequencies are barely detectable in the relatively broad spectrum (e.g., $2f_p = 0.22$ and $3f_p = 0.32$ Hz in Plate 1). The evolution of bispectra observed in 13 m depth during the northeaster are discussed by *Herbers and Guza* [1994]. A 2.83-hour duration bottom-pressure record obtained during the height of the storm in both 8 and 13 m depths is examined here. Spectra, bispectra, and trispectra were calculated by Fourier transforming overlapping (75%), Hanning-windowed, and detided 17-min data segments. The estimates were smoothed over a 0.0156-Hz-wide bandwidth to increase the dof while retaining enough frequency resolution to distinguish the overall spectral features. Consequently, there are approximately 320 dof for the estimates from each sensor. In addition, estimates from several sensors (15 sensors in 13 m depth spanning an area 250 x 250 m, and 10 sensors in 8 m depth spanning an area 200 x 150 m) were averaged. For high-frequency, short-wavelength waves these averages are over independent realizations, but for low-frequency, long-wavelength motions the more closely spaced sensors are not independent. The dof of these estimates therefore varies with frequency, but is roughly 1000. Bi- and trispectra presented below are normalized by the products of the powers (e.g., (1)) of the Fourier components of each triad (bispectra, (2)) or quartet (trispectra, (3)) and are thus a relative measure of the phase coupling between the interacting waves, similar to the bi- and tricoherence. (The statistics of normalized bi- and trispectra are also similar to the corresponding higher-order coherences). *Nikias and Raghuveer* [1987] and *Elgar and Chandran* [1993] review details of the computation, normalization, and statistical fluctuations of higher-order spectra.

Bispectra

The real part of the normalized bottom-pressure bispectrum $B(f_1, f_2)$ of the observations made in 8 m depth indicates phase coupling between pairs of free waves at the primary power spectral peak frequency f_p and forced waves at the first harmonic $2f_p$ ($f_1 = f_2 = f_p = 0.11, f_3 = f_1 + f_2 = 2f_p = 0.22$ Hz in Plate 1b), as well as between waves with frequencies corresponding to the primary, first, and second harmonics ($f_1 = 0.21, f_2 = 0.11, f_3 = 0.32$ Hz in Plate 1b). The imaginary part of $B(f_1, f_2)$ is small relative to the real part (i.e., the biphase ≈ 0, Figures 2a and 2b, discussed below), in agreement with weakly nonlinear theory [*Hasselmann*, 1962; *Hasselmann et al.*, 1963]. Positive real values (yellow/red contours in Plate 1b) are consistent with sum-frequency interactions between directionally collinear free waves [*Hasselmann*, 1962].

Figure 1. Photograph showing two breaking waves (in about 2 and 5 m depths) at the U.S. Army Corps of Engineers' Field Research Facility pier (the deck is about 7.5 m above mean sea level). The surf zone extends more than 1 km offshore. The gages in 8 and 13 m depths are located about 0.2 and 1.2 km offshore from the pier end, respectively.

There is also a positive real peak in $B(f_1, f_2)$ at $f_1 = 0.11, f_2 = 0.11, f_3 = 0.22$ Hz in 13 m depth (yellow/red contours in Plate 1c). However, the pronounced peak in $B(f_1, f_2)$ in 8 m depth at $f_1 = 0.21, f_2 = 0.11, f_3 = 0.32$ Hz (Plate 1b) is absent in 13 m depth (Plate 1c). In 13-m water depth, waves with frequencies greater than about 0.3 Hz forced by nonlinear interactions between directionally collinear free waves have such short wavelengths that they are significantly attenuated at the seafloor. The bottom-pressure field is instead dominated by longer-wavelength waves forced by interactions between obliquely propagating wind waves [*Herbers and Guza*, 1994], for which the real part of $B(f_1, f_2)$ is negative (e.g., note the negative green/blue contours with a maximum at $f_1 = 0.26, f_2 = 0.11, f_3 = 0.37$ Hz in 13 m depth, Plate 1c). Thus the bispectral minimum in 13 m depth (Plate 1c) for $f_3 = 0.32$ Hz may be the result of cancellation of positive contributions from nonlinear interactions between directionally collinear waves (dominant below 0.3 Hz) and negative contributions from interactions between obliquely propagating waves (dominant above 0.35 Hz).

The interactions involving low-frequency (infragravity) waves have negative $B(f_1, f_2)$ in both 8 and 13 m depths (green/blue contours for $f_1 \approx 0.11, f_2 \approx 0.04$ Hz in Plates 2b and 2c), consistent with the theoretical biphase of the interaction between two primary waves (frequencies f_1 and $f_1 + f_2$) and a secondary wave at the small difference frequency $f_2 \ll f_1, f_1 + f_2$ [*Hasselmann et al.*, 1963; *Elgar and Guza*, 1985; *Herbers et al.*, 1994].

The third moments of the wave field, wave skewness and asymmetry, are weighted linear sums of the real and imaginary parts of $B(f_1, f_2)$, respectively. In both 8- and 13-m water depths the dominant $f_p, f_p, 2f_p$ interactions cause positive skewness values (0.42 and 0.14 in 8 and 13 m depths, respectively), significantly different from the zero value of a linear, Gaussian wave field. The corresponding wave asymmetry values (0.07 and -0.001, respectively) are much smaller than the values (0.2-1.0) typically observed in surf zones [*Elgar et al.*, 1990], indicating that the near-bottom-pressure profiles associated with breaking waves in 8 m depth are less pitched forward than is observed in shallower water.

Although not inconsistent with the forcing of a secondary wave by two primary waves, the interpretation of some peaks in the bispectrum is ambiguous. For example, the positive (yellow/red contours) peak at

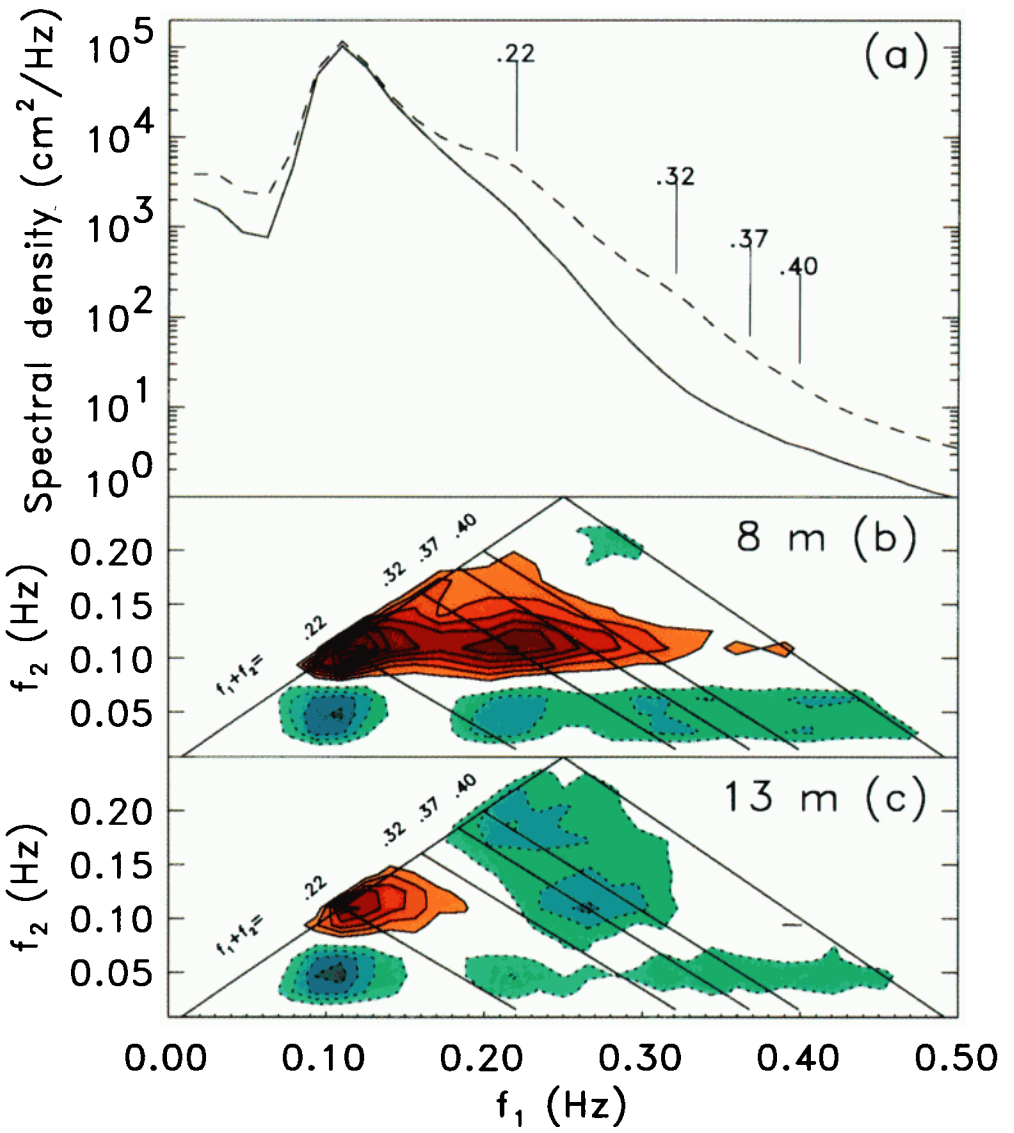

Plate 1. (a) Spectra (dashed curve is 8 m depth, solid curve is 13 m depth) and contours of the real part of the normalized bispectrum of bottom-pressure fluctuations measured in (b) 8- and (c) 13-m water depths. The contours in Plates 1b and 1c indicate phase coupling between waves with frequencies f_1, f_2, and $f_3 = f_1 + f_2$. The minimum contour level is significant at the 90% level, with additional contours at integer multiples of the 90% level, increasing (in magnitude) from yellow to red for positive values and from green to blue for negative values. The four diagonal lines passing through the contours from the $f_1 = f_2$ line to the $f_2 = 0$ axis indicate interactions with sum frequencies $f_1 + f_2 = f_3$ of 0.22, 0.32, 0.37, and 0.40 Hz, as discussed in the text. The same four frequencies are indicated by vertical lines on the spectra in Plate 1a.

$f_1 = 0.21, f_2 = 0.11, f_3 = 0.32$ Hz in 8 m depth (Plate 1b) may involve secondary waves at frequencies close to $3f_p$ (forced by interactions between free waves at f_p and $2f_p$) or tertiary waves (forced by interactions between three free waves near f_p). Similarly, the broad negative (green/blue) peak at $f_1 = 0.26, f_2 = 0.11, f_3 = 0.37$ Hz in 13 m depth (Plate 1c) could involve either secondary or tertiary waves at 0.37 Hz [*Herbers and Guza*, 1994]. The trispectral analysis below confirms the presence of tertiary waves at 0.32 and 0.37 Hz in 8 and 13 m depths, respectively.

Trispectra

The normalized real part of $T(f_1, f_2, f_3)$ is displayed in Plate 2 as contours in (f_1, f_2) space for four fixed values of the sum frequency $f_4 = f_1 + f_2 + f_3$ (the same four sum frequencies are indicated in the corresponding spectra and bispectra shown in Plate 1). The negative values observed for $f_1 \approx f_2 \approx 0.11$ Hz, $f_4 \approx 0.22$ Hz in both 8 (Plate 2a) and 13 (Plate 2e) m depths are consistent with $O(\epsilon^6)$ contributions from phase-coupled quartets consisting of two nearly collinear pri-

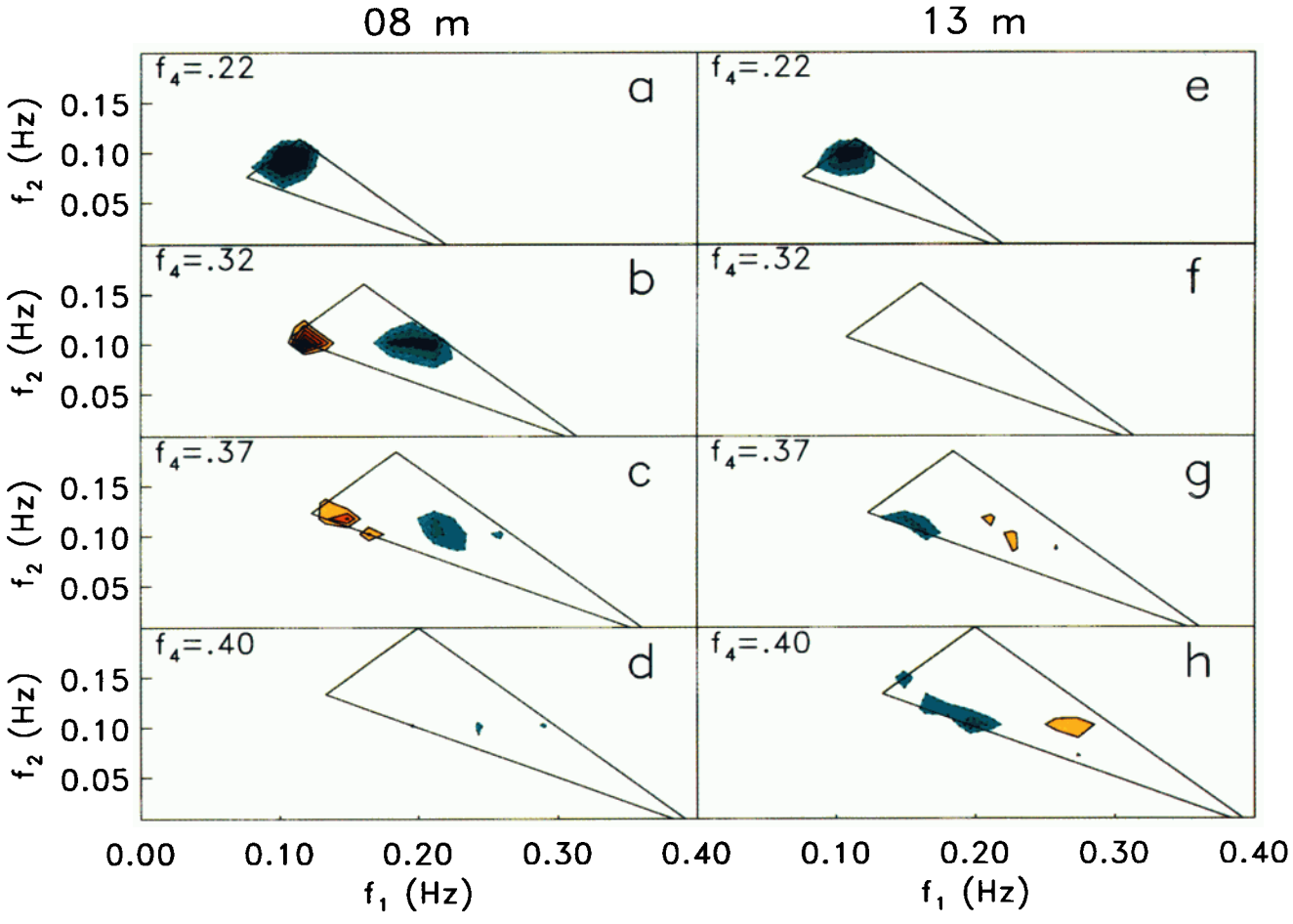

Plate 2. Contours of the real part of the normalized trispectrum of bottom-pressure fluctuations for (a)-(d) 8- and (e)-(h) 13-m water depths. Each panel is for a fixed value of the sum frequency $f_4 = f_1 + f_2 + f_3$, and thus the contours indicate phase coupling between waves with frequencies f_1, f_2, f_4, and $f_3 = f_4 - (f_1 + f_2)$. The triangles drawn in each panel encompass the nonredundant region of (f_1, f_2) space [*Chandran and Elgar*, 1994]. The minimum contour level is significant at the 90% level, with additional contours at integer multiples of the 90% level, increasing (in magnitude) from yellow to red for positive values and from green to blue for negative values. The sum frequencies f_4 are for Plates 2a and 2e, $f_4 = 0.22$ Hz; Plates 2b and 2f, 0.32 Hz; Plates 2c and 2g, 0.37 Hz; and Plates 2d and 2h, 0.40 Hz, and they correspond to the vertical lines on the spectra (Plate 1a) and the diagonal lines on the bispectra (Plates 1b and 1c).

mary waves with frequencies close to the spectral peak ($f_1 \approx f_2 \approx f_p$) and the associated difference-frequency ($f_3 \ll f_1, f_2$) and sum-frequency ($f_4 \approx 2f_p$) secondary waves.

For f_4 close to $3f_p$, in 8 m depth, $T(f_1, f_2, f_3)$ has two peaks ($f_4 = 0.32$ Hz, Plate 2b). The positive (yellow/red) peak for $f_1 \approx f_2 \approx f_3 \approx f_p$ indicates an $O(\epsilon^6)$ contribution of a tertiary wave with frequency $3f_p$ forced by interactions between three directionally nearly collinear waves with frequencies near f_p. The negative trispectral values in Plate 2b possibly are a higher-order ($O(\epsilon^8)$) contribution of a primary wave with frequency $f_2 \approx f_p$, a sum-frequency secondary wave at $f_1 \approx 2f_p$, a difference-frequency secondary wave at $f_3 \ll f_p$, and a sum-frequency tertiary wave at $f_4 \approx 3f_p$. As the sum frequency f_4 increases, the two peaks in $T(f_1, f_2, f_3)$ in 8 m depth weaken (compare Plates 2b and 2c), and are absent for $f_4 \approx 0.4$ Hz (Figure 3*d*). Bispectral levels in 8 m depth also are low at sum frequencies $f_1 + f_2 \geq 0.4$ Hz (Plate 1b).

Tertiary waves are evident as distinct peaks in the 13-m trispectrum for $f_4 = 0.37$ and 0.40 Hz, slightly above $3f_p$ (Plates 2g and 2h, respectively), similar to the peaks in the 8-m trispectrum at slightly lower frequencies (Plates 2b and 2c). However, the signs of the 13-m depth trispectral peaks are opposite those in 8 m because in 13 m depth the short wavelength motions excited by collinear interactions are attenuated over the water column and the trispectrum is dominated by tertiary waves forced by obliquely propagating primary waves. The negative trispectral peak in 13 m depth for $f_4 > 3f_p$ (blue in Plates 2g and 3h) corresponds to $f_2 \approx f_3 \approx f_p$, with f_1 a higher frequency (increasing as f_4 increases). This peak is probably the result of weakly attenuated tertiary waves forced by two collinear waves with frequencies (f_2, f_3) near the primary spec-

tral peak and a higher-frequency (f_1) obliquely traveling wave, qualitatively consistent with the observed directional properties of waves in the swell-sea frequency band during this storm [*Herbers and Guza*, 1994].

The trispectral levels observed in 13 m depth at $f_4 \approx 3f_p$ (Plate 2f) are not statistically significant, possibly owing to cancelling contributions from tertiary waves forced by collinear free waves and tertiary waves forced by obliquely propagating free waves, similar to the transition observed in the bispectrum at $f_3 \approx 0.3$ Hz (Plate 1c).

The imaginary part of the trispectrum in 13 m depth is small and scattered randomly about zero (Figure 2d), as are the imaginary parts of the observed bispectra in both 8 and 13 m depth (Figures 2a and 2b). Vanishing imaginary parts of the bi- and trispectra are consistent with the prediction of third-order nonlinear wave theory that bi- and triphases are either 0 or 180° [*Hasselmann*, 1962, *Herterich and Hasselmann*, 1980]. However, the imaginary part of the trispectrum is larger in 8 m depth (Figure 2c), a deviation from weakly nonlinear wave theory possibly resulting from wave breaking or other strong nonlinearities, but also possibly a measurement error owing to flow noise. Flow noise in 13 m depth was negligible because the sensors were buried about 10 cm in the sandy seabed (see *Herbers and Guza* [1994] and *Herbers et al.* [1992] for further discussion of flow noise).

Summary

The bispectrum has often been used to detect secondary forced waves. The present trispectral analysis of large-amplitude bottom-pressure fluctuations observed in 8-m water depth shows tertiary waves at three times the frequency of the primary power spectral peak forced by three wind-wave components with frequencies near the primary peak. These interactions were not detectable in pressure measurements at the seafloor in 13 m depth, where there is strong vertical decay of these relatively short-wavelength, collinearly forced tertiary waves. On the other hand, the trispectra suggest that weakly attenuated tertiary waves forced by a pair of waves with frequencies near the primary spectral peak and an obliquely propagating higher-frequency wave contribute to the high-frequency bottom-pressure field in 13 m depth. Further work is necessary to quantitatively assess the importance of these interactions.

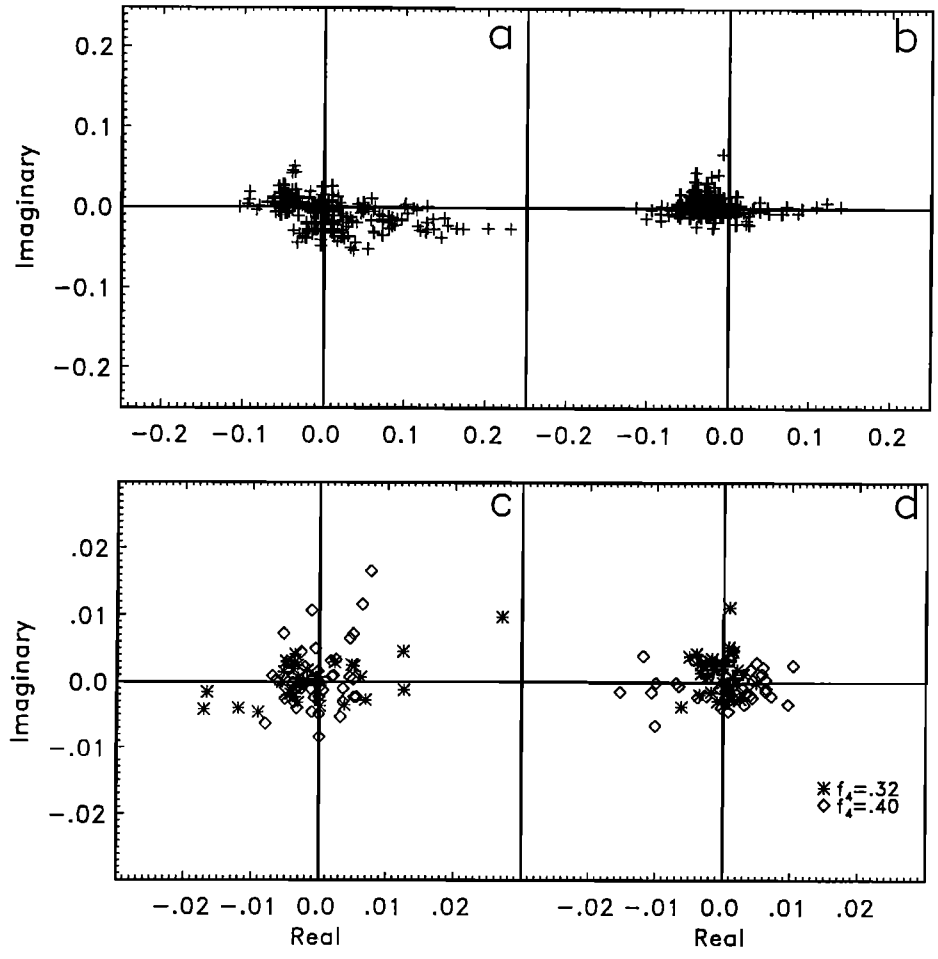

Figure 2. Imaginary versus real parts of normalized (a) 8-m depth bispectrum, (b) 13-m depth bispectrum, (c) 8-m depth trispectrum, and (d) 13-m depth trispectrum. Values are shown for all possible triads (pluses) in the bispectra and for quartets with $f_4 = 0.32$ Hz (stars) and $f_4 = 0.40$ Hz (diamonds) in the trispectra.

Acknowledgments. This research was supported by the Office of Naval Research (Nonlinear Ocean Waves ARI and Coastal Dynamics). The Field Research Facility, Coastal Engineering Research Center, Duck, N.C. contributed valuable data and logistical support.

References

Barrick, D., and B. Lipa, The second-order shallow-water hydrodynamic coupling coefficient in interpretation of HF radar sea echo, *IEEE J. Oceanic Eng., 11*, 310–315, 1986.

Bowen, A. J., Simple models of nearshore sedimentation; beach profiles and longshore bars; in *The Coastline of Canada*, pp. 21-30, Geological Survey of Canada, Ottawa, Ont., 1980.

Brillinger, D., and M. Rosenblatt, Asymptotic theory of kth-order spectra, in *Advanced Seminar on Spectral Analysis of Time Series*, edited by B. Harris, pp. 153-188, John Wiley, New York, 1967.

Chandran, V., and S. Elgar, Mean and variance of estimates of the bispectrum of a harmonic random process: An analysis including effects of spectral leakage, *IEEE Trans. Signal Process., 39*, 2640–2651, 1991.

Chandran, V., and S. Elgar, A general procedure for the derivation of principal domains of higher-order spectra, *IEEE Trans. Signal Process., 42*, 229–233, 1994.

Chandran, V., S. Elgar, and B. Vanhoff, Statistics of tricoherence, *IEEE Trans. Signal Process., 42*, 3430-3440, 1994.

Donelan, M.E., J. Hamilton, and W.H. Hui, Directional spectra of wind generated waves, *Philos. Trans. R. Soc. London A, 315*, 509–562, 1985.

Elgar, S., and V. Chandran, Higher-order spectral analysis to detect nonlinear interactions in measured time series and an application to Chua's circuit, *Int. J. Bifurcation and Chaos, 3*, 19–34, 1993.

Elgar, S., and R.T. Guza, Observations of bispectra of shoaling surface gravity waves, *J. Fluid Mech., 161*, 425–448, 1985.

Elgar, S., and R.T. Guza, Nonlinear model predictions of bispectra of shoaling surface gravity waves, *J. Fluid Mech., 167*, 1–18, 1986.

Elgar, S., and G. Sebert, Statistics of bicoherence and biphase, *J. Geophys. Res., 94*, 10,993–10,998, 1989.

Elgar, S., M.H. Freilich, and R.T. Guza, Model-data comparisons of moments of nonbreaking shoaling surface gravity waves, *J. Geophys. Res., 95*, 16,055–16,063, 1990.

Elgar, S., T.H.C. Herbers, M. Okihiro, J. Oltman-Shay, and R.T. Guza, Observations of infragravity waves, *J. Geophys. Res., 97*, 15,573–15,577, 1992.

Hasselmann, K., On the non-linear energy transfer in a gravity-wave spectrum, I, General theory, *J. Fluid Mech., 12*, 481–500, 1962.

Hasselmann, K., W. Munk, and G. MacDonald, Bispectra of ocean waves, in *Time Series Analysis*, edited by M. Rosenblatt, pp. 125–139, John Wiley, New York, 1963.

Haubrich, R.A. Earth noises, 5 to 500 millicycles per second, *J. Geophys. Res., 70*, 1415–1427, 1965.

Herbers, T.H.C., and R.T. Guza, Wind-wave nonlinearity observed at the sea floor, I, Forced-wave energy, *J. Phys. Oceanogr., , 21*, 1740–1761, 1991.

Herbers, T.H.C., and R.T. Guza, Wind-wave nonlinearity observed at the sea floor, II, Wavenumbers and third-order statistics, *J. Phys. Oceanogr., 22*, 489–504, 1992.

Herbers, T.H.C., and R.T. Guza, Nonlinear wave interactions and high-frequency sea floor pressure, *J. Geophys. Res., 99*, 10,035–10,048, 1994.

Herbers, T.H.C., R.L. Lowe, and R.T. Guza, Field observations of orbital velocities and pressure in weakly nonlinear surface gravity waves, *J. Fluid Mech., 245*, 413–435, 1992.

Herbers, T.H.C., S. Elgar, and R.T. Guza, Infragravity-frequency (0.005-0.05 Hz) motions on the shelf, I, Forced waves, *J. Phys. Oceanogr., 24*, 917–927, 1994.

Herterich, K., and K. Hasselmann, A similarity relation for the nonlinear energy transfer in a finite-depth gravity-wave spectrum, *J. Fluid Mech., 97*, 215–224, 1980.

Kim, Y.C., and E.J. Powers, Digital bispectral analysis and its applications to nonlinear wave interactions, *IEEE Trans. Plasma Sci., 7*, 120–131, 1979.

Longuet-Higgins, M.S., A theory of the origin of microseisms, *Philos. Trans. R. Soc. London A, 243*, 1–35, 1950.

Longuet-Higgins, M.S., and R.W. Stewart, Radiation stresses in water waves: A physical discussion, with applications, *Deep Sea Res., 11*, 529–562, 1964.

Nikias, C.L., and M. R. Raghuveer, Bispectrum estimation: A digital signal processing framework, *Proc. IEEE, 75*, 867–891, 1987.

Phillips, O.M., On the dynamics of unsteady gravity waves of finite amplitude, 1, *J. Fluid Mech. 9*, 193–217, 1960.

Vinod Chandran, School of Electrical and Electronic Systems Engineering, Queensland University, GPO Box 2434, Brisbane, QLD 4001, AUSTRALIA.

Steve Elgar, Electrical Engineering and Computer Science, Washington State University, Pullman, WA 99164-2752. (e-mail: elgar@eecs.wsu.edu)

R.T. Guza, Center for Coastal Studies 0209, University of California, La Jolla, CA 92093.

T.H.C. Herbers, Department of Oceanography, Naval Postgraduate School, Monterey, CA 93943.

(Received May 17, 1994; revised November 7, 1994; accepted November 7, 1994.)